

# Wavelet Based Satellite Image Change Detection Using Level Sets Algorithm

Mr. P. Ramesh.<sup>1</sup>

Assistant Professor .MLRIT.

Mr. D. Naresh kumar<sup>2</sup>

Assistant Professor. MLRIT.

Mr. M. Srikanth<sup>3</sup>.

Assistant Professor. MLRIT.

## Abstract

*In this paper satellite image change detection can done by using level sets algorithm for to get robustness against noise, wavelet transform is exploited to obtain a multi resolution representation of the difference image, which is obtained from two satellite images acquired from the same geographical area but at different time instances. A Level set algorithm is then applied to the multi resolution representation of the difference image for segment the difference image into the "changed" and "unchanged" regions. The proposed change detection method has been conducted on satellite images . The simulation results clearly show that the proposed change detection method using level sets algorithm gives good performance compared to Fourier analysis .*

## I. INTRODUCTION

Digital image processing is an area characterized by the need for extensive experimental work to establish the viability of proposed solutions to a given problem. An important characteristic underlying the design of image processing systems is the significant level of testing & experimentation that normally is required before arriving at an acceptable solution. This characteristic implies that the ability to formulate approaches & quickly prototype candidate solutions generally plays a major role in reducing the cost & time required to arrive at a viable system implementation.

An image may be defined as a two-dimensional function  $f(x, y)$ , where  $x$  &  $y$  are spatial coordinates, & the amplitude of  $f$  at any pair of coordinates  $(x, y)$  is called the intensity or gray level of the image at that point. When  $x$ ,  $y$  & the amplitude values of  $f$  are all finite discrete quantities, we call the image a digital image. The field of DIP refers to processing digital image by means of digital computer. Digital image is composed of a finite number of elements, each of which has a particular location & value. The elements are called pixels.

Vision is the most advanced of our sensor, so it is not surprising that image play the single most

important role in human perception. However, unlike humans, who are limited to the visual band of the EM spectrum imaging machines cover almost the entire EM spectrum, ranging from gamma to radio waves. They can operate also on images generated by sources that humans are not accustomed to associating with image.

There is no general agreement among authors regarding where image processing stops & other related areas such as image analysis & computer vision start. Sometimes a distinction is made by defining image processing as a discipline in which both the input & output at a process are images. This is limiting & somewhat artificial boundary. The area of image analysis (image understanding) is in between image processing & computer vision.

There are no clear-cut boundaries in the continuum from image processing at one end to complete vision at the other. However, one useful paradigm is to consider three types of computerized processes in this continuum: low-, mid-, & high-level processes. Low-level process involves primitive operations such as image processing to reduce noise, contrast enhancement & image sharpening. A low-level process is characterized by the fact that both its inputs & outputs are images. Mid-level process on images involves tasks such as segmentation, description of that object to reduce them to a form suitable for computer processing & classification of individual objects. A mid-level process is characterized by the fact that its inputs generally are images but its outputs are attributes extracted from those images. Finally higher- level processing involves "Making sense" of an ensemble of recognized objects, as in image analysis & at the far end of the continuum performing the cognitive functions normally associated with human vision. Digital image processing, as already defined is used successfully in a broad range of areas of exceptional social & economic value.

### A. Image Introduction

An image is represented as a two dimensional function  $f(x, y)$  where  $x$  and  $y$  are spatial co-ordinates and the amplitude of ' $f$ ' at any pair of coordinates  $(x, y)$  is called the intensity of the image at that point.

## B. Gray scale image

A grayscale image is a function  $I$  (xylem) of the two spatial coordinates of the image plane.  $I(x, y)$  is the intensity of the image at the point  $(x, y)$  on the image plane.  $I$  (xylem) takes non-negative values assume the image is bounded by a rectangle  $[0, a] \times [0, b]$ :  $I: [0, a] \times [0, b] \rightarrow [0, \text{info}]$

## C. Color image

It can be represented by three functions,  $R$  (xylem) for red,  $G$  (xylem) for green and  $B$  (xylem) for blue. An image may be continuous with respect to the  $x$  and  $y$  coordinates and also in amplitude. Converting such an image to digital form requires that the coordinates as well as the amplitude to be digitized. Digitizing the coordinate's values is called sampling. Digitizing the amplitude values is called quantization.

## D. Coordinate convention

The result of sampling and quantization is a matrix of real numbers. We use two principal ways to represent digital images. Assume that an image  $f(x, y)$  is sampled so that the resulting image has  $M$  rows and  $N$  columns. We say that the image is of size  $M \times N$ . The values of the coordinates (xylem) are discrete quantities. For notational clarity and convenience, we use integer values for these discrete coordinates. In many image processing books, the image origin is defined to be at  $(x, y) = (0, 0)$ . The next coordinate values along the first row of the image are  $(x, y) = (0, 1)$ . It is important to keep in mind that the notation  $(0, 1)$  is used to signify the second sample along the first row. It does not mean that these are the actual values of physical coordinates when the image was sampled. Following figure shows the coordinate convention. Note that  $x$  ranges from 0 to  $M-1$  and  $y$  from 0 to  $N-1$  in integer increments.

The coordinate convention used in the toolbox to denote arrays is different from the preceding paragraph in two minor ways. First, instead of using (xylem) the toolbox uses the notation (r, c) to indicate rows and columns. Note, however, that the order of coordinates is the same as the order discussed in the previous paragraph, in the sense that the first element of a coordinate tuple, (r, c), refers to a row and the second to a column. The other difference is that the origin of the coordinate system is at  $(r, c) = (1, 1)$ ; thus,  $r$  ranges from 1 to  $M$  and  $c$  from 1 to  $N$  in integer increments. IPT documentation refers to the coordinates. Less frequently the toolbox also employs another coordinate convention called spatial coordinates which uses  $x$  to refer to columns and  $y$  to refer to rows. This is the opposite of our use of variables  $x$  and  $y$ .

## II. WAVELETS

### A. FOURIER ANALYSIS

Signal analysts already have at their disposal an impressive arsenal of tools. Perhaps the most well-known of these is Fourier analysis, which breaks down a signal into constituent sinusoids of different frequencies. As shown in Fig (1) Another way to think of Fourier analysis is as a mathematical technique for transforming our view of the signal from time-based to frequency-based.

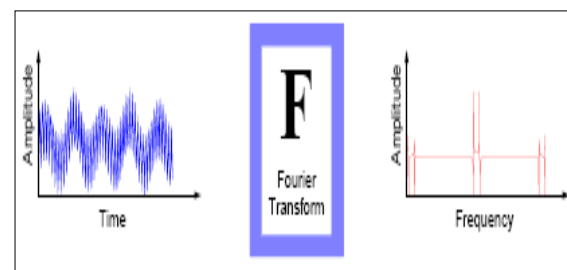


Fig (1)

For many signals, Fourier analysis is extremely useful because the signal's frequency content is of great importance. So why do we need other techniques, like wavelet analysis?

Fourier analysis has a serious drawback. In transforming to the frequency domain, time information is lost. When looking at a Fourier transform of a signal, it is impossible to tell when a particular event took place. If the signal properties do not change much over time — that is, if it is what is called a stationary signal — this drawback isn't very important. However, most interesting signals contain numerous non stationary or transitory characteristics: drift, trends, abrupt changes, and beginnings and ends of events. These characteristics are often the most important part of the signal, and Fourier analysis is not suited to detecting them.

### B. SHORT-TIME FOURIER ANALYSIS:

In an effort to correct this deficiency, Dennis Gabor (1946) adapted the Fourier transform to analyze only a small section of the signal at a time — a technique called windowing the signal. Gabor's adaptation, called the Short-Time Fourier Transform (STFT), as shown in Fig (2) maps a signal into a two-dimensional function of time and

frequency.

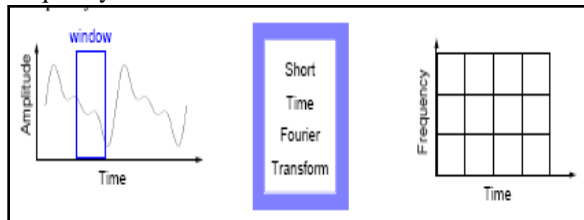
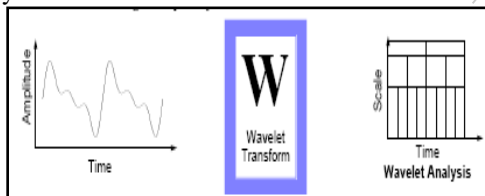


Fig (2)

The STFT represents a sort of compromise between the time- and frequency-based views of a signal. It provides some information about both when and at what frequencies a signal event occurs. However, you can only obtain this information with limited precision, and that precision is determined by the size of the window. While the STFT compromise between time and frequency information can be useful, the drawback is that once you choose a particular size for the time window, that window is the same for all frequencies. Many signals require a more flexible approach—one where we can vary the window size to determine more accurately either time or frequency.

### C.WAVELET ANALYSIS

Wavelet analysis represents the next logical step: a windowing technique with variable-sized regions. Wavelet analysis allows the use of long time intervals where we want more precise low-frequency information, and shorter regions where we want high-frequency information.



Fig(3)

As shown in Fig (3) Here's what this looks like in contrast with the time-based, frequency-based, and STFT views of a signal:

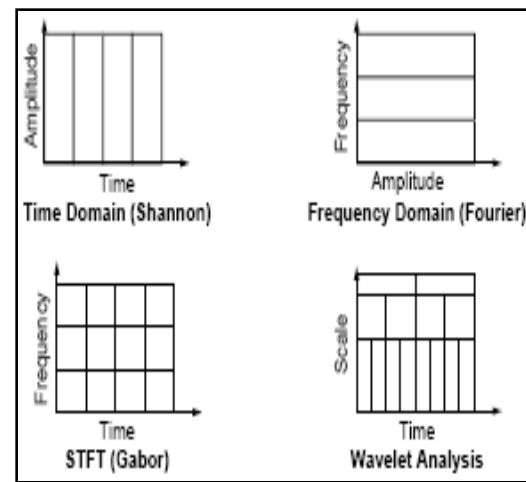


Fig (4)

You may have noticed that in Fig (4) wavelet analysis does not use a time-frequency region, but rather a time-scale region. For more information about the concept of scale and the link between scale and frequency, see "How to Connect Scale to Frequency?"

### III. LEVEL -SET ALGORITHM

#### A.PROBLEM FORMULATION:

Let  $X_1$  and  $X_2$  be two co-registered multi temporal remote sensing images acquired over the same geographical area at two different times. Let  $X$  be the scalar  $M \times N$  difference image generated from  $X_1$  and  $X_2$  by applying the change vector analysis technique CVA [11]. The aim of the proposed approach is to generate a change-detection map representing the changes occurred between the two acquisition dates of the two images. To this end, we propose to formulate this issue as a segmentation problem and solve it by means of a variational level set method.

A well known segmentation model is the one proposed by Mumford-shah aiming at finding a contour  $C$  which segments the difference image  $X$  into non overlapping regions associated with changed and unchanged classes, respectively.

The related energy functional is given by:

$$F^{MS}(I, C) = \int_{\Omega} |X - I|^2 dx dy + \lambda \int_{\Omega/C} |\nabla I|^2 dx dy + \mu |C| \quad (1)$$

Where  $\Omega$  is the image domain,  $|C|$  is the length of the contour  $C$ ,  $\lambda$  and  $\mu$  are positive

parameters. The minimization of Mumford-Shah functional results in an optimal contour that segments the difference image  $X$ , in addition to an image  $I$  formed from smooth regions within each of the connected components in the image domain separated by the optimal contour  $C$ .

The minimization of the above functional is difficult in practice as it is a non convex problem. A possible solution is to consider the special case where the image  $I$  in the functional (1) is a piecewise constant function. In this case, the energy functional is given by:

$$F^{MS}(C, c1, c2) = \int_{inside(C)} |X - c1|^2 dx dy + \int_{outside(C)} |X - c2|^2 dx dy + \mu |C| \quad (2)$$

The functional (2) is known as the piecewise constant Mumford-Shah segmentation model or Chan-Vase model [12].

We call the two terms in (2) the global fitting energy. The parameter  $\mu$  controls the trade-off between the goodness-of-fit and the length of the curve  $C$ .  $c1$  and  $c2$  are two constants that approximate the image  $X$  in the segments inside( $C$ ) and outside( $C$ ) respectively. For a fixed contour  $C$ , the optimal values for these parameters are given by the average of  $X$  over the regions inside( $C$ ) and outside( $C$ ).

In order to minimize the above functional, we adopt a level-set formulation.

## B.LEVEL-SET FORMULATION:

In the level-set method the curve  $C$  is represented by the zero level set of a Lipschitz function  $\phi : \Omega \rightarrow \mathbb{R}$  such that:

$$C = \partial\omega = \{(x, y) \in \Omega : \phi(x, y) = 0\},$$

$$Inside(C) = \omega = \{(x, y) \in \Omega : \phi(x, y) > 0\},$$

$$Outside(C) = \Omega \setminus \bar{\omega} = \{(x, y) \in \Omega : \phi(x, y) < 0\}, \quad (3)$$

By replacing the unknown variable  $C$  by the level-set function  $\phi$ , we obtain :

$$F^{MS}(\phi, c1, c2) = \int_{\Omega} |X - c1|^2 H(\phi) dx dy + \int_{\Omega} |X - c2|^2 (1 - H(\phi)) dx dy + \mu \int_{\Omega} |\nabla H(\phi)| dx dy \quad (4)$$

where  $H$  is the Heaviside function and it is approximated in practice by the smooth function  $H_{\epsilon}$  defined by:

$$H_{\epsilon}(Z) = 1/2(1 + 2/\pi \arctan(z/\epsilon))$$

(5)

The minimization of the functional (4) with respect to the level-set function  $\phi$  and the two constants  $c1$  and  $c2$  can be done according to the iterative approach adopted in [12].

Step 1: Set  $k=0$  and initialize  $\phi$  by  $\phi^k$

Step 2: For  $\phi = \phi^k$ , compute  $c_1^k$  and  $c_2^k$  as the averages of  $X$  in  $\phi > 0$  and  $\phi \leq 0$ , respectively:

Step 3: compute  $\phi^{k+1}$  by solving the following partial differential equation:

$$\phi^{k+1} = \phi^k - \Delta t \frac{\partial F^{MS}}{\partial \phi}(\phi^{k-1}, c_1^k, c_2^k)$$

Where  $\Delta t$  is the time step

Step 4: Reinitialize  $\phi$  locally to the signed distance function to the curve.

Step 5: End the process if the convergence is reached;

Otherwise go to step 2

**IV. SOURCE CODE**

```

clc;
clear all;
close all;
I11=imread('ALASKA_1985_321.jpg');
I1=rgb2gray(I11);
figure,imshow(I1);title('Original image at time T1');
I1=im2double(I1);
I22=imread('ALASKA_2005_321.jpg');
I2=rgb2gray(I22);
I2=imresize(I2,[size(I1)]);
figure,imshow(I2);title('Original image at time T2');
I2=im2double(I2);
x=zeros(size(I1));
for r=1:length(I1)
    for c=1:length(I2)
        x(r,c)=abs(I2(r,c)-I1(r,c));
    end
end
for r=1:length(I1)
    for c=1:length(I2)
        x(r,c)=((x(r,c)-min(min(x)))./(max(max(x))-min(min(x))).*255;
    end
end
save x
figure,imshow(x),title('differnce image');
[x,S]=myswt(x,1,'haar');
figure,imshow(x),title('wavelet output image');
x1=x(1:S(1,1),1:S(1,2));
c1=0.0732;
c2=0.6310;
lm1=0.05;
lm2=0.09;
for r=1:S(1,1)
    for c=1:S(1,2)
        vp(r,c)=(lm1*(x1(r,c)-c1)^2+lm2*(x1(r,c)-c2)^2+0.5*length(x1));
    end
end
m=mean(mean(vp));
for r=1:S(1,1)
    for c=1:S(1,2)
        if vp(r,c)<=m
            out(r,c)=1;
        else
            out(r,c)=0;
        end
    end
end
figure,imshow(out),title('OUTPUT IMAGE AFTER SEGMENTATION')

```

## V. SIMULATION RESULTS

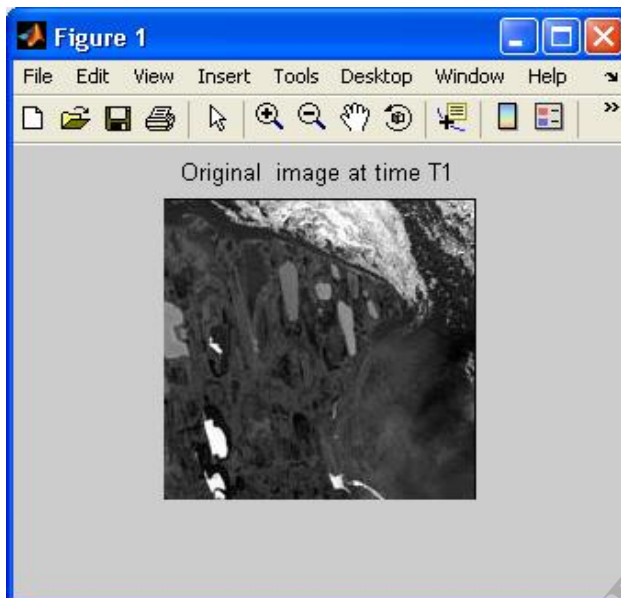


Fig.1:Original image at time T1

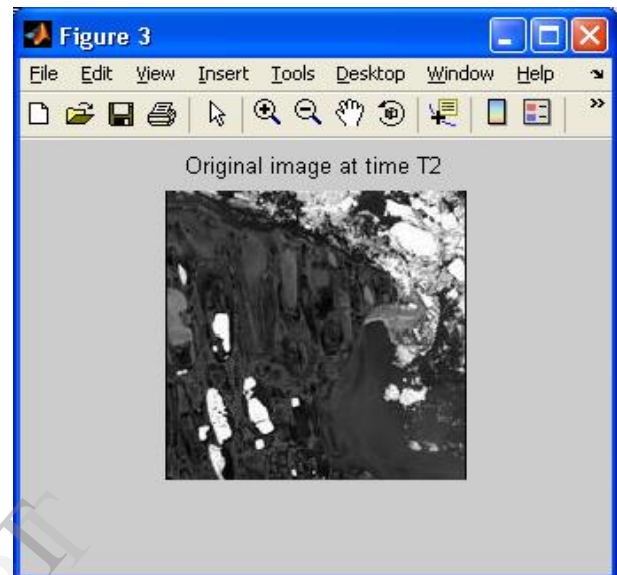


Fig.3: Original image at time T2

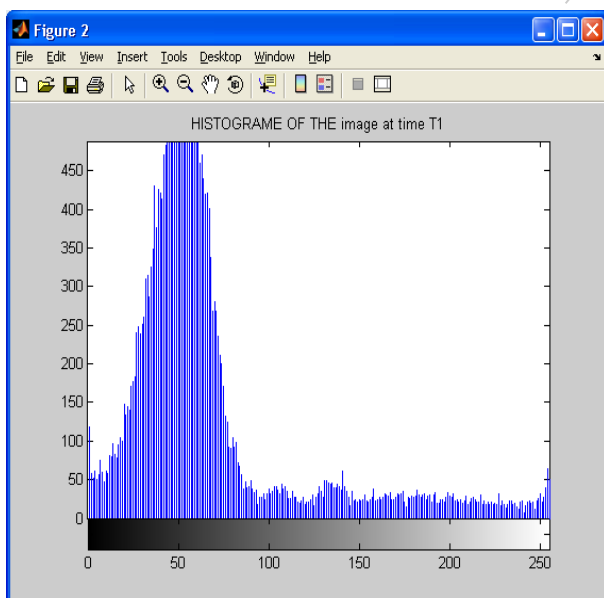


Fig.2: Histogram of the image at T1

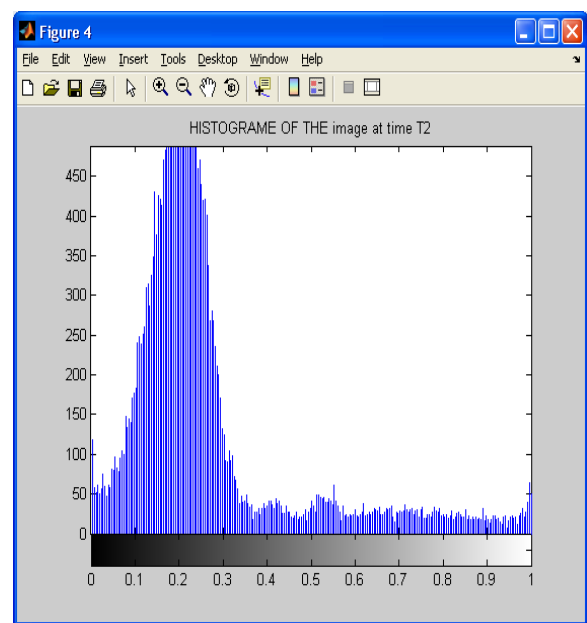


Fig.4: Histogram of the image time T2

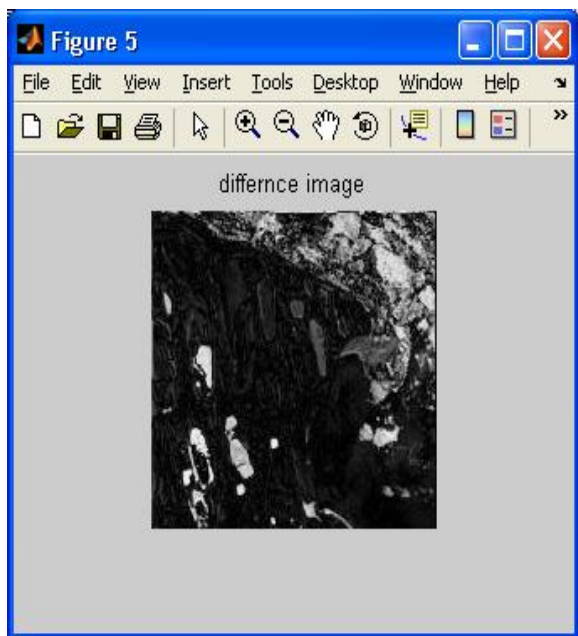


Fig5:Difference image.

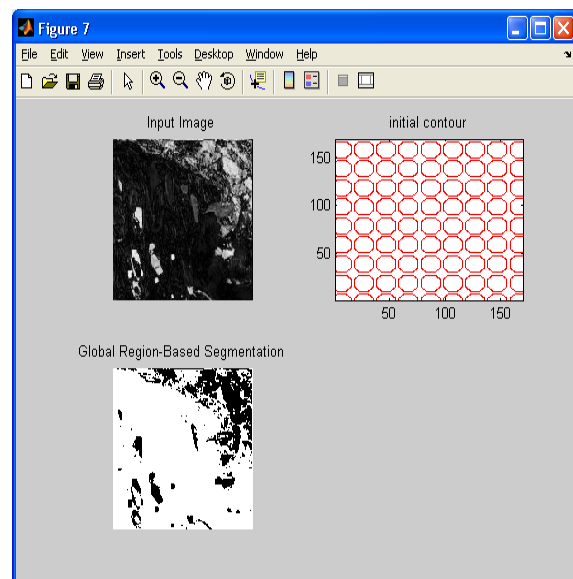


Fig.7: Global region based segmentation

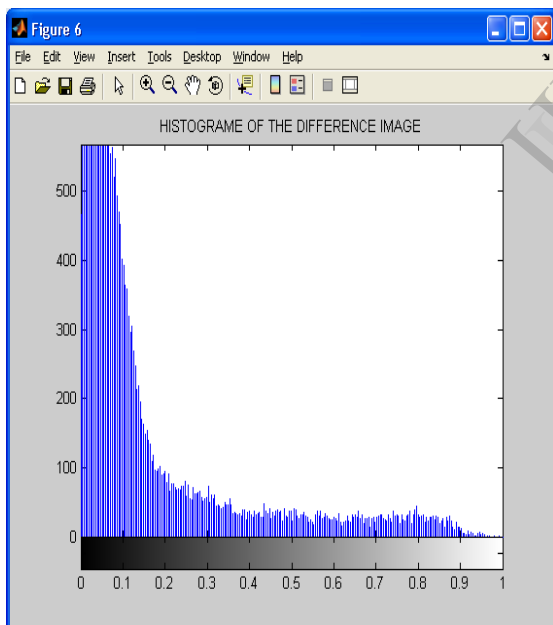


Fig 6: Histogram of the difference image

## VI.EXPERIMENTAL RESULTS



Fig: Alaska 1



Fig: Alaska 2

### CONCLUSION:

In this paper satellite image change detection can be done by using level sets algorithm and compared with the experimental results, wavelet transform is exploited to obtain a multi resolution representation of the difference image, which is obtained from two satellite images acquired from the same geographical area but at different time instances. A Level set algorithm is then applied to the multi resolution representation of the difference image for segment the difference image into the "changed" and "unchanged" regions. The proposed change detection method has been conducted on satellite images and by using MATLAB tool simulation results verified and corresponding generated images were shown. These images shows the difference of changes in satellite images.

### REFERENCES

- [1] M. Torma, P. Harma, and E. Jarvenpaa, "Change detection using spatial data problems and challenges," in *Proc. IEEE Int. Geosci. Remote Sens. Symp.*, Jul. 2007, pp. 1947–1950.
- [2] S. Leprince, S. Barbot, F. Ayoub, and J.-P. Avouac, "Automatic and precise orthorectification, coregistration, and subpixel correlation of satellite images, application to ground deformation measurements," *IEEE Trans. Geosci. Remote Sens.*, vol. 45, no. 6, pp. 1529–1558, Jun. 2007.
- [3] C. Shah, Y. Sheng, and L. Smith, "Automated image registration based on pseudoinvariant metrics of dynamic land-surface features," *IEEE Trans. Geosci. Remote Sens.*, vol. 46, no. 11, pp. 3908–3916, Nov. 2008.
- [4] L. Bruzzone and D. Prieto, "Automatic analysis of the difference image for unsupervised change detection," *IEEE Trans. Geosci. Remote Sens.*, vol. 38, no. 3, pp. 1171–1182, May 2000.
- [5] T. Kasetkasem and P. Varshney, "An image change detection algorithm based on Markov random field models," *IEEE Trans. Geosci. Remote Sens.*, vol. 40, no. 8, pp. 1815–1823, Aug. 2002.
- [6] T. Celik, "Unsupervised change detection in satellite images using principal component analysis and  $k$ -means clustering," *IEEE Geosci. Remote Sens. Lett.*, vol. 6, no. 4, pp. 772–776, Oct. 2009.
- [7] F. Bovolo and L. Bruzzone, "A detail-preserving scale-driven approach to change detection in multitemporal SAR images," *IEEE Trans. Geosci. Remote Sens.*, vol. 43, no. 12, pp. 2963–2972, Dec. 2005.
- [8] T. Celik and K.-K. Ma, "Unsupervised change detection for satellite images using dual-tree complex wavelet transform," *IEEE Trans. Geosci. Remote Sens.*, vol. 48, no. 3, pp. 1199–1210, Mar. 2010.